Crystallization Kinetics for Simulation of Processing of Various Polyesters

Kyuk Hyun Kim, Avraam I. Isayev, Keehae Kwon

Institute of Polymer Engineering, The University of Akron, Akron, Ohio 44325-0301

Received 30 August 2005; accepted 10 April 2006
DOI 10.1002/app.24630
Published online in Wiley InterScience (www.interscience.wiley.com).

ABSTRACT: The approach to determine crystallization kinetic parameters based on the DSC nonisothermal crystallization experiments is applied to poly(butylene terephthalate) (PBT) and poly(ethylene-2,6-naphthalate) (PEN). The differential form of the Nakamura equation and master curve approach are used. The isothermal induction times are obtained from nonisothermal induction times according to the concept of induction time index. The correction of temperature lag between the DSC furnace and the sample is incorporated. The corrected nonisothermal crystallization kinetic data is shifted with respect to an arbitrarily chosen reference temperature to obtain the master curve. By fitting the obtained master curve with the Hoffman-Lauritzen equation, the model parameters for the crystallization rate constant are obtained. The relative crystallinity measured at different cooling and heating rates is described by these model parameters. © 2006 Wiley Periodicals, Inc. J Appl Polym Sci 102: 2847–2855, 2006

Key words: crystallization; kinetics; polyesters; master curve approach

INTRODUCTION

In various polymer processing operations, different degrees of crystallization occur in different positions of the part as a result of the nonuniform temperature distribution created by the rapid cooling and the heat of crystallization. The mechanical properties of the product are influenced by the developed microstructure, which is determined by the extent of crystallization. Therefore, it is very important to take into account the crystallization kinetics in the process modeling of crystallizing polymers.

For isothermal crystallization, the overall crystallization kinetics has been widely described by the Avrami–Kolmogoroff equation.[1,2] For nonisothermal crystallization, a number of mathematical models have been proposed based on this equation. Ozawa[3] has developed an equation to analyze nonisothermal crystallization by introducing a cooling rate term into the kinetic equation. However, the Ozawa equation is not suitable in process modeling because a constant cooling rate is assumed. Nakamura et al.[4,5] have extended the Avrami equation to describe nonisothermal crystallization kinetics, customarily called the ''Nakamura model,'' on the basis of isokinetic assumptions that the number of activated nuclei is independent of temperature and that the nucleation rate and the growth rates follows the same time dependence. Schneider et al.[6] proposed differential first-order rate equations for describing the nonisothermal crystallization kinetics by combining the work of Avrami.[1] Chan and Isayev[7] considered the problems and difficulties involved in the prediction of nonisothermal crystallization kinetics based on the isothermal data alone. The differential form of the Nakamura equation and the rate of crystallization as a function of temperature in Hoffman–Lauritzen equation[8] were used. They showed good agreement between the nonisothermal crystallinity results obtained from DSC experiments and the predicted data. Chan et al.[9] tried to obtain the model parameters of crystallization kinetics based on the nonisothermal experimental data using a shift factor. The kinetic data was corrected for the effects of temperature lag between the DSC sample and furnace using the Eder and Janeschitz-Kriegl approach[10,11] that was based on experimental data alone without resorting to any kinetic model.

Several studies of the crystallization kinetics have been done for various polyesters, including polyethylene terephthalate (PET),[7,9,12,13] polybutylene terephthalate (PBT),[14] and polyethylene-2,6-naphthalate (PEN).[15–17] Most of these studies were developed based on the modification of the Avrami equation. Chan et al.[7,9] proposed a method to obtain the nonisothermal crystallization kinetic parameters based on the isothermal[7] and nonisothermal[9] experiments for PET. Zhang and Cao[13] derived a kinetic equation for nonisothermal crystallization by extending the Avrami equation. A few studies have been carried out on isothermal[14,16,17] and nonisothermal[15] crystallization kinetics

Correspondence to: A. I. Isayev (aisayev@uakron.edu).
Contract grant sponsor: Divison of Engineering, National Science Foundation; contract grant number: DMI-0322920.

for PBT and PEN. Bian et al.[14] investigated the isothermal crystallization kinetics of PET, PBT, and various copolymers and determined the crystallization rate constant and the Avrami exponents. Lee and Cakmak[15] used the models proposed by Ozawa and Nakamura to describe the nonisothermal crystallization kinetics of PEN. All these studies were carried out without a correction for temperature lag and in a narrow range of temperatures being insufficient for use in simulation of polymer processing.

To simulate the polymer processing of semicrystalline polymers, such as extrusion and injection molding, the crystallization kinetic data is required to determine the developed crystallinity and thickness of the flow-induced crystallized layer. In the present study, parameters of crystallization kinetic model for two polyesters, PBT and PEN, over a wide range of temperatures, are determined based on the nonisothermal DSC experiments corrected for temperature lag and compared with earlier data obtained on PET.[7,9] The nonisothermal crystallization kinetic data obtained by DSC experiments are shifted to obtain a master curve for crystallization kinetics. By fitting the master curve, the model parameters for the crystallization rate constant are obtained and are suitable for the modeling of injection molding with flow-induced crystallization proposed earlier.[18] Here, Nakamura equation with the Hoffman–Lauritzen equation is used to calculate the crystallinity developed during cooling or heating experiments and compared with the measured data for PBT and PEN samples. The kinetic data obtained here will be used for simulation of injection molding of polyesters in the later publication.

THEORETICAL

Nonisothermal crystallization kinetics

Nakamura et al.[4,5] extended the Avrami–Kormogoroff equation to describe nonisothermal crystallization kinetics. In the differential form, this equation is

$$\frac{d\theta}{dt} = nK(T)(1-\theta)[-\ln(1-\theta)]^{(n-1)/n} \tag{1}$$

where θ is the relative degree of crystallinity; n, the Avrami exponent. The quiescent nonisothermal crystallization rate constant, $K(T)$ is described by the Hoffman–Lauritzen equation[8] as

$$K(T) = (\ln 2)^{1/n}\left(\frac{1}{t_{1/2}}\right)_0 \exp\left(\frac{-U^*/R}{T-T_\infty}\right)\ \exp\left(-\frac{K_k}{T(T_m^0-T)f}\right) \tag{2}$$

with $T_\infty = T_g - 30$, $f = \dfrac{2T}{T+T_m^0}$,

where T_m^0 is the equilibrium melting temperature; f is the correction factor for the reduction in the latent heat of fusion as the temperature is decreased; R, the universal gas constant; U^*, the activation energy for segmental jump of polymer molecules, assigned a universal value of 6284 J/mol; $t_{1/2}$, the half-time of crystallization; K_k, the nucleation exponent.

The original Nakamura equation makes no allowance for the induction time for nucleation. Following the approach of Sifleet et al.,[19] nonisothermal induction times can be obtained from isothermal induction time as

$$\bar{t} = \int_0^{t_I} \frac{dt}{t_i(T)} = 1 \tag{3}$$

where $t_i(T)$ is the isothermal induction time as a function of temperature. When the value of the dimensionless induction time index, $\bar{t}$, reaches unity, the upper limit of integration is taken as the nonisothermal induction time, t_I.

For cold crystallization, t_i is assumed to follow an Arrhenius-type temperature dependence as

$$t_i = t_c\ \exp\left(\frac{T_0}{T}\right) \tag{4}$$

where t_c and T_0 are material constants independent of the temperature T.

For melt crystallization, an expression for t_i[20] is used

$$t_i = \frac{t_m}{(T_m^0 - T)^a} \tag{5}$$

where t_m and a are material constants independent of the temperature T.

Master curve approach to crystallization kinetics

A master curve approach to determine crystallization kinetics described earlier[9] was used to determine the crystallization rate constant from the nonisothermal DSC experimental data. From the heat of fusion of DSC, plots of the relative crystallinity, θ, and rate of crystallization, $\frac{d\theta}{dt}$, versus temperature at different cooling rates can be obtained as shown schematically in Figure 1. The shift factor at a constant degree of crystallinity, θ_j, is expressed as

$$\frac{(d\theta/dt)_{ij}}{(d\theta/dt)_{rj}} = \frac{K(T_{ij})f(\theta_j)}{K(T_{rj})f(\theta_j)} = \frac{K(T_{ij})}{K(T_{rj})} = a_T(T_{ij}) \tag{6}$$

where $a_T(T_{ij})$ is the shift factor at temperature T_{ij} with respect to the reference temperature, T_{rj} for the

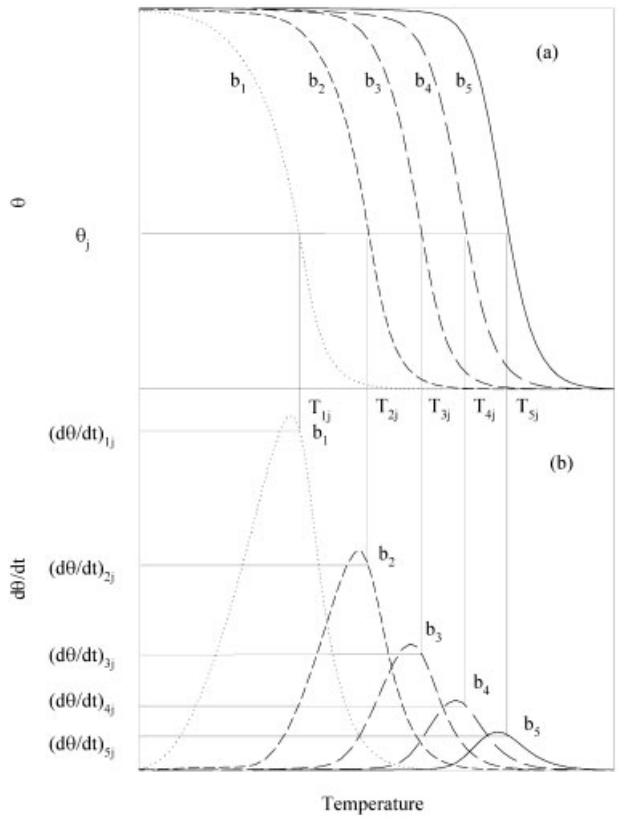

Figure 1 Schematic plots of evolution of degree of crystallinity (a) and the rate of crystallization (b) at different cooling rates.

*i*th cooling rate and the *j*th degree of crystallinity. By shifting the function, $a_T(T_{ij})$, in the vertical direction with respect to the constant reference crystallinity, θ_r, the shift factor function is then

$$a_T(T) = \frac{K(T)}{K(T_r)} \tag{7}$$

By fitting the master curve of eq. (7) with eq. (2), the material constants, K_k and $(t_{1/2})_0$ will be determined. Also, the Avrami constant, n, can be calculated from plotting the relative crystallinity with respect to the time. Therefore, the crystallization kinetics can be expressed by eqs. (1) and (2) using calculated constants.

Temperature lag between DSC sample and furnace

Because of the heat transfer barriers between the DSC furnace and the pan, and between the pan and the sample, there is a temperature lag between the furnace and the sample in nonisothermal experiments. The temperature measured by DSC is not the sample temperature, but the furnace temperature. Therefore, an equation for estimating the temperature lag between the sample and the furnace in nonisothermal experiments proposed by Wu et al.[21] was used as

$$-(m_sC_s + m_aC_a)\frac{dT}{dt} + m_s\Delta H_f X_\infty \frac{d\theta}{dt} = hA(T - T_f) \tag{8}$$

where m and C are the mass and specific heat, where subscripts s and α denote the sample and aluminum pen, respectively; T and T_f are the temperature of sample and furnace, respectively; h is the heat transfer coefficient between the pan (containing the sample) and the furnace; and A is the area of the heat transfer surface. Product of hA can be obtained by indium calibration of DSC.

A criterion for the applicability of eq. (8) can be obtained by defining a modified Nusselt number:

$$Nu^* = \frac{hL}{k_{\text{th}}} \tag{9}$$

where L and k_{th} are the thickness and heat conductivity of the sample, respectively. Equation (8) can be used to determine the temperature lag between the sample and the furnace if the modified Nusselt number is less than unity.[10] The calculated Nusselt number for PBT and PEN samples, as shown below, were 0.31 and 0.43, respectively. Since the Nusselt number is less than 1, eq. (8) can be applied for the temperature lag calculations.

EXPERIMENTAL

Two polyesters, polybutylene terephthalate (PBT) and polyethylene-2,6-naphthalate (PEN), were used. PBT, Ultradur KR 4036-Q692, was provided by BASF AG (Wyandotte, MI), and PEN, VFR-40046PEN, was supplied by Shell Chemical Company (Houston, Texas). Some fundamental properties of these samples are listed in Table I.

TA DSC, DSC-Q100, was used to perform the nonisothermal crystallization experiments. The calibration was done by using indium, sealed in aluminum pans. The indium sample was heated from 25 to 180°C at the rate of 20°C/min. For cooling experiments, each sample prepared from pellets was heated from room temperature to around 30°C above the melting temperature and annealed for 10 min to remove the previous thermal history. Then, the sample was cooled down at various cooling rates, 2.5, 5, 10, 20, and 40°C/min for PBT and 1.25, 2.5, 5, 10, and 15°C/min for PEN by using the

TABLE I
Fundamental Properties of Materials

	PBT	PEN
IV (dL/g)	1.24	0.64
T_g (°C)	55[22]	110[23]
ΔH_m^0(kJ/mol)	32.0[23]	25.0[23]
T_m^0(°C)	245[23]	337[23]

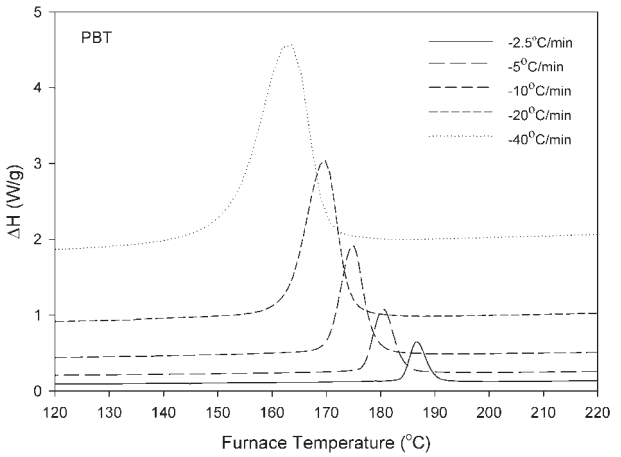

Figure 2 Heat flow curves of the nonisothermal crystallization of PBT at various cooling rates.

liquid nitrogen. Also, the heating experiments for PEN samples were done at various heating rates, 1.25, 2.5, 5, and 10°C/min. Similar heating and cooling experiments were done to get the baseline by using empty pans in both reference and sample compartments of DSC. The baseline was subtracted from the experimental heat flow curve at the same cooling rate.

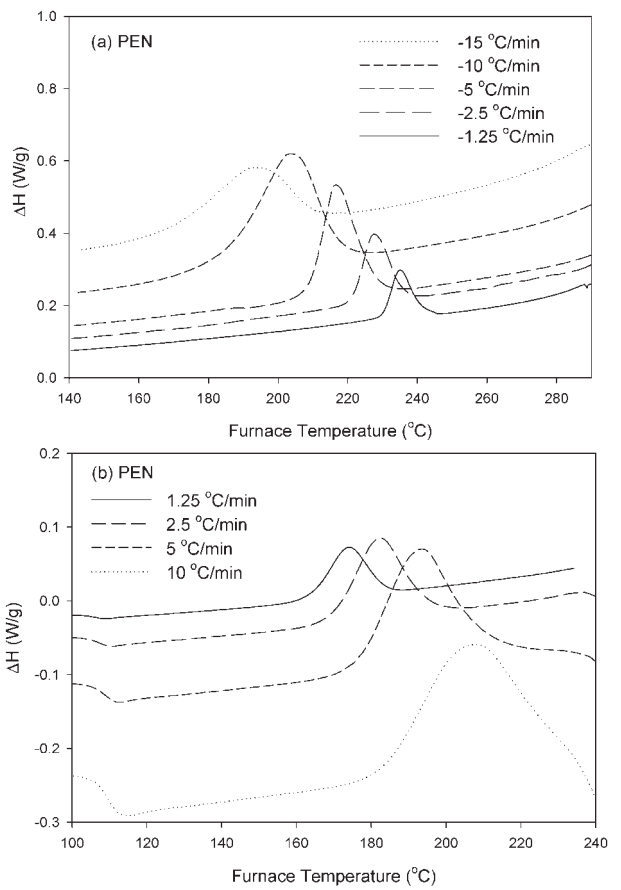

Figure 3 Heat flow curves of the nonisothermal crystallization of PEN at various cooling (a) and heating (b) rates.

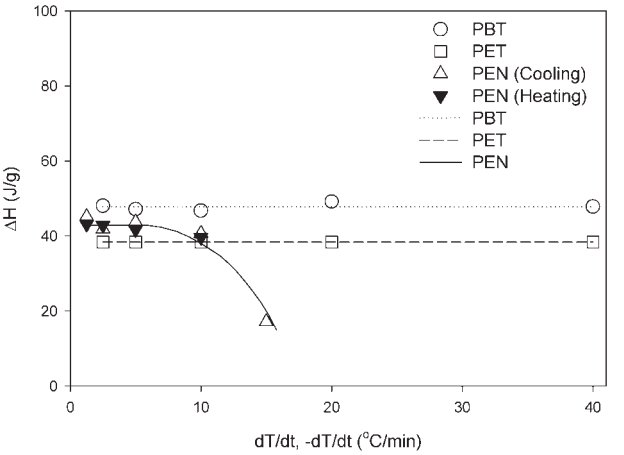

Figure 4 Total heat release of the nonisothermal crystallization of PBT and PET[7] at various cooling rates, and PEN at various cooling and heating rates.

RESULTS AND DISCUSSION

Heat flow curves

Figures 2 and 3(a) show the typical heat flow (normalized to the weight of the samples) curves of the nonisothermal crystallization of PBT and PEN at various cooling rates, respectively. Figure 3(b) illustrates the heat flow curve of the nonisothermal crystallization of PEN at various heating rates. As results, Figure 4 shows the total heat release of the nonisothermal crystallization of PBT (cooling), PET (cooling),[7] and PEN (cooling and heating). Ultimate crystallinity, X_∞, was calculated based on ΔH in Figure 4 and values of ΔH_m^0, heat of fusion of a perfect crystal, given in Table I for PBT and PEN. Generally, as the cooling rate increases, the peak and starting temperatures for crystallization decrease [Figs. 2 and 3(a)]. Results are typical of nonisothermal crystallization[24] and were also

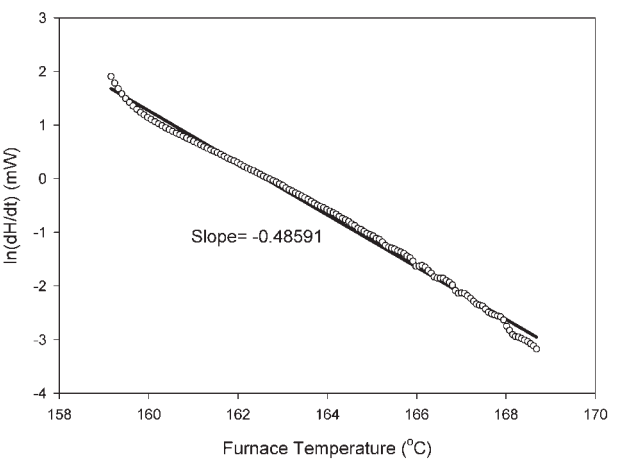

Figure 5 Evaluation of heat transfer coefficient between the aluminum and furnace from the high temperature decay side of the heat flow curve.

TABLE II
Material Properties for Temperature Lag Correction

Quantity	PBT samples	PEN samples	Aluminum pan
m (mg)	5.2	4.6	56.8
A (m^2)	28.26×10^{-6}	28.26×10^{-6}	28.26×10^{-6}
L (m)	1.965×10^{-4}	1.965×10^{-4}	–
C (J kg^{-1} K^{-1})	2.14×10^{3} [27]	2.17×10^{3} [27]	8.97×10^{2} [28]
k_{th} (J $s^{-1}m^{-1}K^{-1}$)	1.750×10^{-1} [29]	2.300×10^{-1} [29]	2.37×10^{2} [28]
hA (J/K)	8.45×10^{-3}	8.45×10^{-3}	–
Nu*	0.31	0.43	–

obtained for PET[25] and PP,[26] respectively. This is due to the degree of supercooling, which is the driving force for crystallization.[24] At higher cooling rates, the degree of supercooling is higher, which allows the polymer chains less time to crystallize. Because of the greater amount of time at the slower cooling rate, the polymer chains have a greater chance to transform to higher degrees of crystallinity. As shown in Figure 4, the total heat release of PBT and PET does not depend on the cooling rate, whereas that of PEN decreases when the cooling (or heating) rate increases, especially at the cooling rate of 15°C/min. This finding can be explained as follows. PET and PBT crystallize faster than PEN. Thus, at the cooling rates used in the present study, the heat release of PET and PBT is not a function of cooling rate. However, because of the bulkiness of polymer chains of PEN, its crystallization process is very slow. In particular, if time for crystallization is not sufficient, as typically occurs at high heating or cooling rate, complete crystallization of PEN is not possible. Therefore, its crystallinity, instead of increasing, is reduced. Furthermore, at very high heating or cooling rate, the condition could be attained such that PEN would not crystallize at all and would rather vitrify into the amorphous state. This explains reduction of the heat release of PEN at a cooling rate of 15°C/min as shown in Figures 3(a) and 4.

Temperature lag correction

The DSC heat flow curve of the indium calibration was obtained. Indium calibration is used not only to calibrate the heat flow but also to obtain the overall heat transfer coefficient between the DSC furnace and the pan for the temperature lag correction. The overall heat transfer coefficient obtained from the slope of the plot of $\ln\frac{dH}{dt}$ as a function of furnace temperature is –0.48591 J K^{-1} s^{-1} as shown in Figure 5. The necessary data for calculation of the overall heat transfer coefficient is listed in Table II. The temperature lag between the sample and the furnace for PBT and PEN during cooling experiments is given in Figures 6 and 7(a), respectively. The temperature lag for PEN during heating experiments is given in Figure 7(b). It is seen from these figures that a faster cooling or heating rate will give a larger temperature lag.

Induction time from nonisothermal experiments

Figures 8 and 9 show the measured and calculated nonisothermal induction times at different cooling and heating rates, respectively. The nonisothermal induction time is calculated according to the concept of induction time index in eq. (3). Corresponding experimental data was obtained from nonisothermal DSC experiments. The material constants are $t_m = 9.46 \times 10^{18}$ s and $a = 9.333$ for melt crystallization of PBT, $t_c = 4.50 \times 10^{-13}$ s and $T_o = 1.245 \times 10^4$ K for cold crystallization of PEN, and $t_m = 5.59 \times 10^{20}$ s and $a = 5.336$ for melt crystallization of PEN. From Figures 8 and 9, it can be seen that eq. (3) fits the nonisothermal induction times quite well.

Master curve approach for nonisothermal crystallization

Figures 10 and 11 show the relative crystallinity, θ, as a function of the sample temperature for PBT and PEN, respectively, after the temperature lag correction

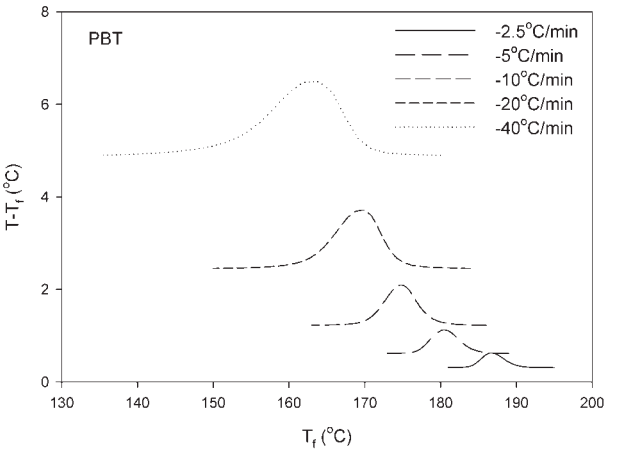

Figure 6 Temperature lag correction between the sample temperature (T) and DSC furnace temperature (T_f) for PBT in cooling experiments.

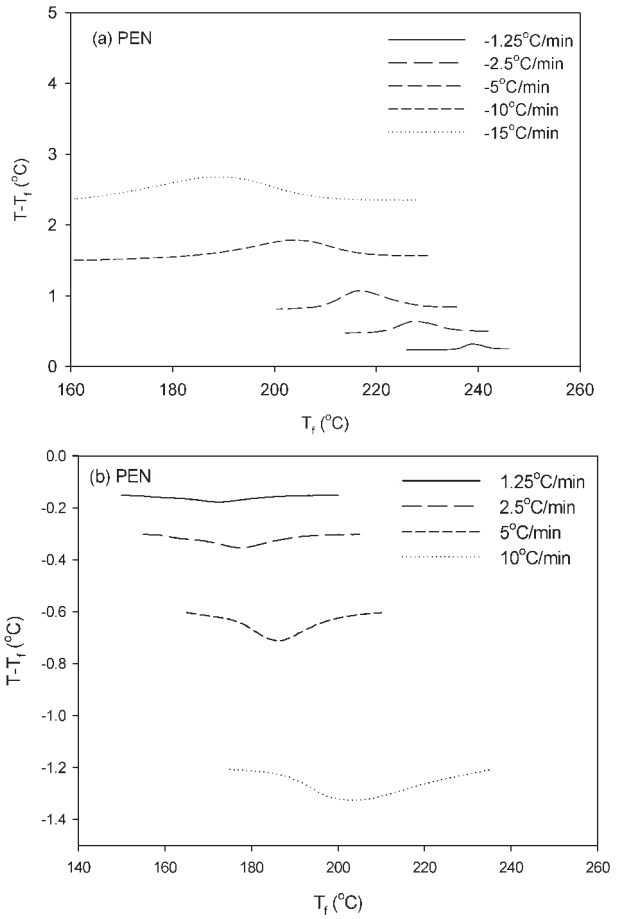

Figure 7 Temperature lag correction between the sample temperature (T) and DSC furnace temperature (T_f) for PEN in cooling (a) and heating (b) experiments.

at different cooling rates. In addition, Figure 12 illustrates the relative crystallinity, θ, at different heating rates for PEN corrected for the temperature lag. Induction times determined by eq. (3) are incorporated.

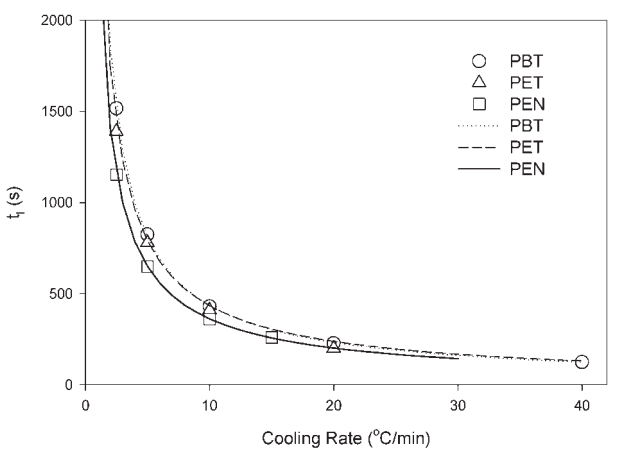

Figure 8 The measured (symbols) and predicted (lines) nonisothermal induction times as a function of cooling rate for PBT, PET,[7] and PEN.

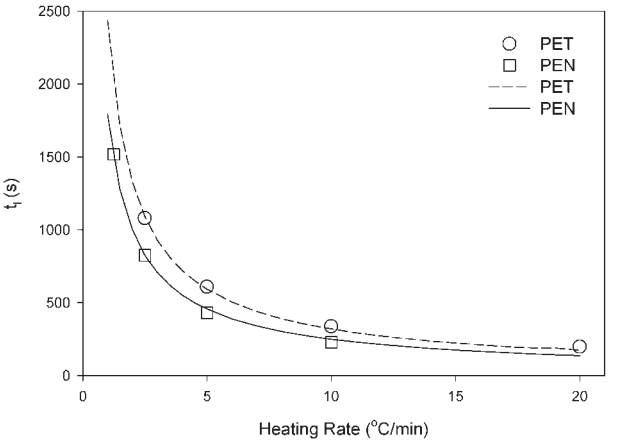

Figure 9 The measured (symbols) and predicted (lines) nonisothermal induction times as a function of heating rate for PET[7] and PEN.

As seen from Figures 10 and 11, the measured and predicted crystallinity coincides well up to –20°C/min in case of PBT, and up to –10°C/min in case of PEN. However, lack of the fit is evident at higher cooling rates. This deviation is more significant for PEN, which is a slow crystallizing polymer. Presently, a complete explanation of this deviation is not possible. However, it is clear that when the PEN melt cools down very fast, it does not have sufficient time for crystallization. In other words, because of the lack of crystallization time, the PEN melt at this high cooling rate has already passed through the temperature corresponding to the highest crystallization rate, as indicated by the bell-shaped curve in Figure 17 below. In this case, cold crystallization at higher cooling rates may not provide accurate information about crystallization kinetics. Therefore, the melt crystallization upon heating from room temperature is more desirable. Accordingly, the lack of the

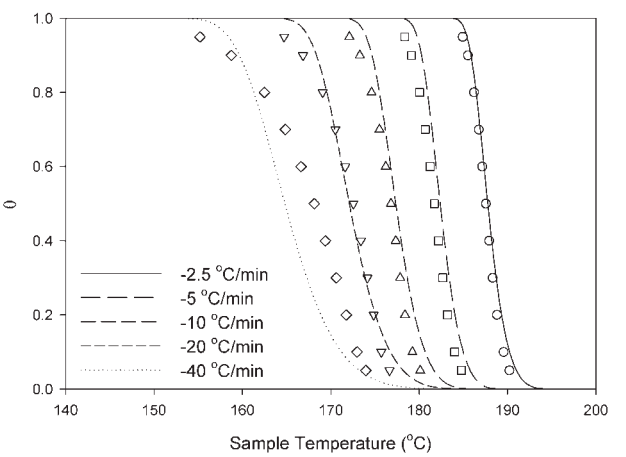

Figure 10 The measured (symbols) and predicted (lines) relative crystallinity as a function of sample temperature at various cooling rates for PBT.

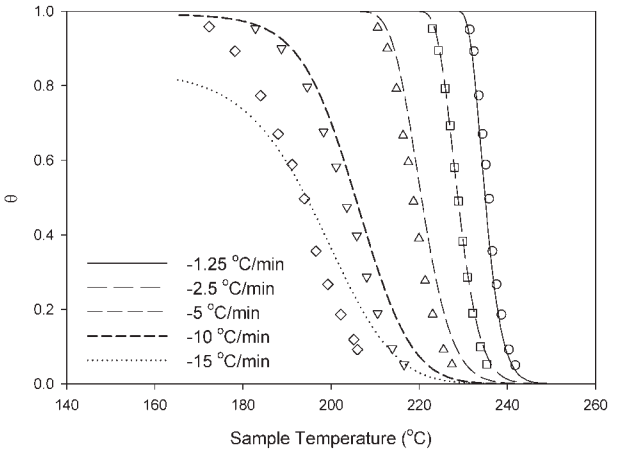

Figure 11 The measured (symbols) and predicted (lines) relative crystallinity as a function of sample temperature at various cooling rates for PEN.

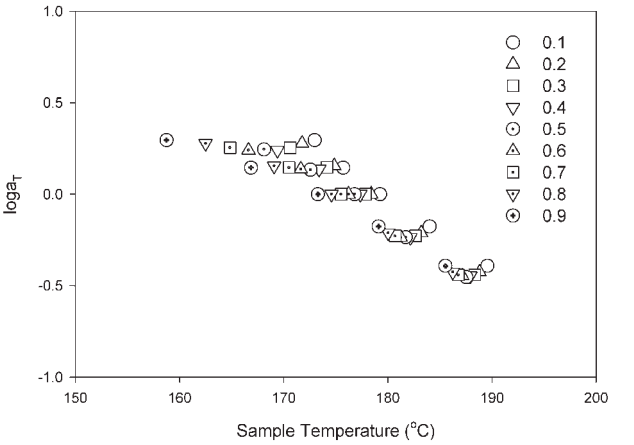

Figure 13 Shift factors as a function of temperature at various degrees of crystallinity for PBT in cooling experiments.

fit between the measured and predicted crystallinity at higher cooling rate does not mean that the model would not be adequate for application to polymer processing (extrusion, injection molding, and fiber spinning) taking place at high cooling rates. In fact, this model was applied to PEN injection molding.[29] In agreement with experiments, the model indicated that PEN moldings do not crystallize at all under typical molding conditions, as obtained in molding experiments.

To get more accurate crystallization kinetic parameters, the data obtained at cooling and heating experiments should be combined. Therefore, heating experiments were carried out in case of PEN. Then, both cooling and heating experiments were combined together to predict overall crystallization kinetics. The measured and predicted relative crystallinity of PEN at a heating rate of 10°C/min was well fitted, as illustrated in Figure 12.

As indicated in schematic Figure 1, on the curves of θ versus T for each material, the line of constant degree of crystallinity is drawn at different cooling rates. This is typically done at θ = 0.1, 0.2, 0.3, 0.4, 0.5, 0.6, 0.7, 0.8, 0.9. Then, the corresponding values of T_{ij} and $\left(\frac{d\theta}{dt}\right)_{ij}$ [i = cooling rates (1–5), j = crystallinity (1–9)] are evaluated. For each θ_j, the reference temperatures, T_{rj}, are chosen as T_{3j} at cooling rate of 10°C/min for PBT and T_{2j} at a cooling or heating rate of 2.5°C/min for PEN. Therefore, the corresponding shift factor, $a_T(T_{ij})$, is determined by using eq. (6). The obtained shift factors, $a_T(T_{ij})$, as a function of the sample temperature are shown in Figures 13 and 14 for cooling experiments of PBT and for cooling and heating experiments of PEN, respectively. Then by taking the curve with $\theta_j = 0.5$ as the overall reference curve and shifting all the other curves along the log a_T axis with respect to the reference curve, the master curves of log a_T versus T are obtained as shown in

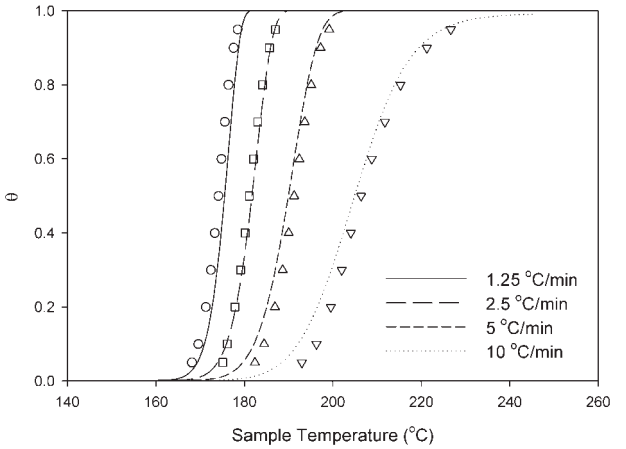

Figure 12 The measured (symbols) and predicted (lines) relative crystallinity as a function of sample temperature at various heating rates for PEN.

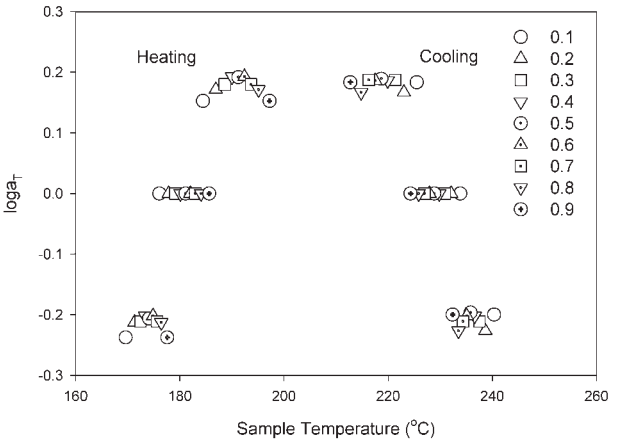

Figure 14 Shift factors as a function of temperature at various degrees of crystallinity for PEN in cooling and heating experiments.

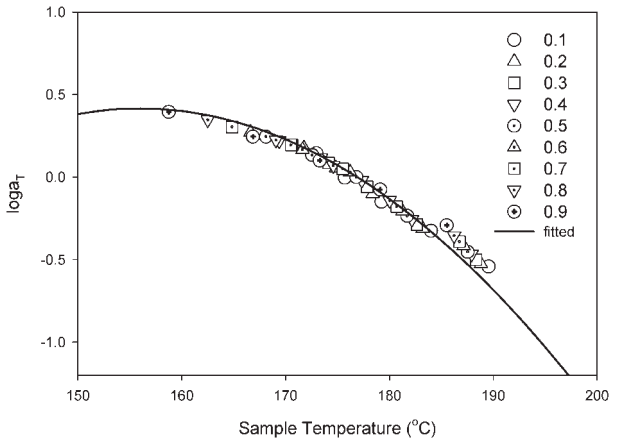

Figure 15 Master curve of shift factor as a function of temperature for PBT in cooling experiments.

Figures 15 and 16. The reference temperatures, 176.8°C for PBT, 228.9°C for PEN cooling, and 182.0°C for PEN heating experiment are chosen to compare each material. By fitting the master curve of Figures 15 and 16 by eq. (7), with the Hoffman–Lauritzen crystallization kinetic equation, eq. (2), the kinetic constants, K_k and $(t_{1/2})_0$, can be determined. Then the nonisothermal crystallization rate was calculated by using the obtained kinetic constants. The results of these calculations are shown in Figure 17 by lines. For comparison, the calculated crystallization rate for PP[26] and PET[9] are shown. Figure 17 illustrates that PBT shows a higher crystallization rate than PET[9] or PEN, and PET shows a higher crystallization rate than PEN. Moreover, the obtained crystallization rates of various polyesters (PBT, PET, and PEN) are lower than that of PP.[26] This is due to the fact that molecular chains are easier to arrange in PBT compared to PET and PEN, and in PET compared to PEN because of their molecular structure. The difficulty of the arrangement of molecular chains becomes strong in the case of PEN

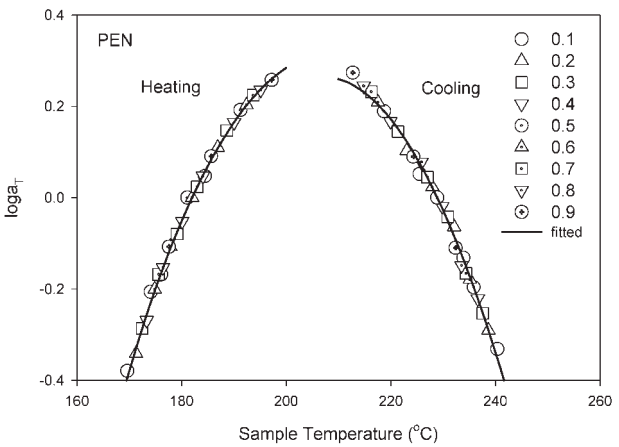

Figure 16 Master curve of shift factor as a function of temperature for PEN in cooling and heating experiments.

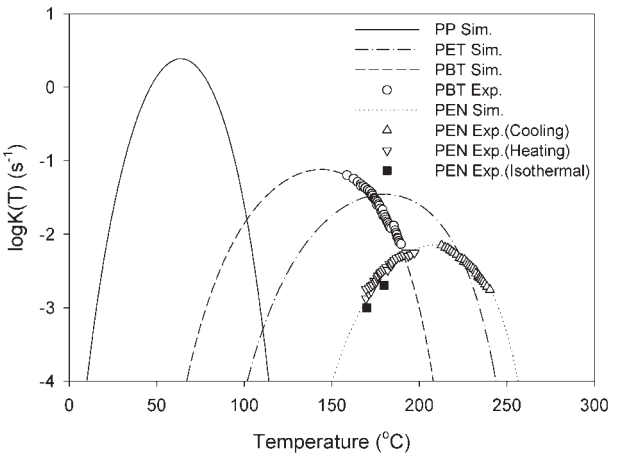

Figure 17 The measured (symbols) and predicted (lines) nonisothermal crystallization rate for PP,[26] PET,[9] PBT, and PEN.

because of the presence of the bulky naphthalene structure in the molecular chain. To verify the obtained kinetic constants, the isothermal experiments at 170 and 180°C for PEN were carried out. These two data points are illustrated in Figure 17. Clearly, they are close to the crystallization rate obtained by nonisothermal crystallization experiments.

The calculated relative crystallinity (lines) by using Nakamura equation, eq. (1), are compared with the measured data (symbols) in Figures 10 and 11 for various cooling rates for PBT and PEN, respectively. Crystallinity development is well predicted by using the obtained material constants in Hoffman–Lauritzen equation with the incorporation of induction time, although as the cooling rate becomes higher, a discrepancy starts to occur. Similarly, the measured (symbols) and predicted (lines) relative crystallinity at various heating rates for PEN are shown in Figure 12 and are found to be in good agreement. Therefore, the Hoffman–Lauritzen equation is suitable to use to predict the nonisothermal crystallization kinetics of various polyesters over a wide range of temperatures, which is otherwise unattainable through experiments. The obtained material constants for crystallization kinetics are $K_k = 2.68 \times 10^5 K^2$ and $(t_{1/2})_0 = 3.38 \times 10^4\ s^{-1}$ for PBT and $K_k = 1.98 \times 10^5 K^2$ and $(t_{1/2})_0 = 8.94 \times 10^2\ s^{-1}$ for PEN.

CONCLUSIONS

The crystallization kinetic parameters were obtained based on the nonisothermal DSC experiments for PBT and PEN samples. The crystallization rate parameters in Hoffman–Lauritzen equation are obtained based on the master curve approach. The temperature lag between the furnace and the sample due to the heat transfer barriers between the DSC furnace and the

pan, and between the pan and the sample is calculated to obtain the sample temperature. The nonisothermal crystallization kinetic data corrected for temperature lag are shifted with respect to an arbitrary reference temperature to obtain the master curve. By fitting the master curve of crystallization kinetic data, the model parameters for Hoffman–Lauritzen equation were obtained. Two isothermal experimental data points for PEN sample were obtained to verify the nonisothermal crystallization kinetic data. The comparison of the nonisothermal crystallization rate between various polyesters including PET, in which the crystallization kinetic was obtained earlier,[9] was made. PBT showed a higher crystallization rate than the PET or PEN samples. The predicted relative crystallinity based on the Nakamura equation with the incorporation of nonisothermal induction time was compared with the experimental data and found to be in good agreement. These crystallization kinetic data will be used for description of crystallization behavior during injection molding.

References

1. Avrami, M. J Chem Phys 1939, 7, 1103.
2. Kolmogoroff, A. N. Izv Akad Nauk SSSR Ser Math 1937, 1, 355.
3. Ozawa, T. Polymer 1971, 12, 150.
4. Nakamura, K.; Watanabe, T.; Katayama, K.; Amano, T. J Appl Polym Sci 1972, 16, 1077.
5. Nakamura, K.; Katayama, K.; Amano, T. J Appl Polym Sci 1973, 17, 1031.
6. Schneider, W.; Koppl, A.; Berger, J. Int Polym Proc 1988, 2, 151.
7. Chan, T. W.; Isayev, A. I. Polym Eng Sci 1994, 34, 461.
8. Hoffman, J. D.; Davis, G. T.; Lauritzen, S. I. Treatise on Solid State Chemistry, Vol. 3: Crystalline and Non-crystalline Solids; Hannay, N. B., Ed.; Plenum: New York, 1976.
9. Chan, T. W.; Shyu, G. D.; Isayev, A. I. Polym Eng Sci 1995, 35, 733.
10. Eder, G.; Janeschitz-Kriegl, H.; Liedauer, S. Prog Polym Sci 1990, 15, 629.
11. Janeschitz-Kriegl, H.; Wippel, H.; Paulik, C.; Eder, G. Colloid Polym Sci 1993, 271, 1107.
12. Kim, K. J.; Ko, S. W. J Korea Fiber Soc 1985, 22, 338.
13. Zhang, Z.; Cao, Z. Chin J Polym Sci 1990, 8, 142.
14. Bian, J.; Ye, S. R.; Feng, L. X. Gaodeng Xuexiao Huaxue Xuebao 2000, 21, 1481.
15. Lee, S. W.; Cakmak, M. J Macromol Sci Phys 1998, 37, 501.
16. Hu, Y. S.; Rogunova, M.; Schiraldi, D. A.; Hiltner, A.; Baer, E. J Appl Polym Sci 2002, 86, 98.
17. Lee, W. D.; Yoo, S. E.; Im, S. S. Polymer 2003, 44, 6617.
18. Kim, K. H.; Isayev, A. I.; Kwon, K. J Appl Polym Sci 2005, 95, 502.
19. Sifleet, W. L.; Dinos, N.; Collier, J. R. Polym Eng Sci 1973, 13, 10.
20. Godovsky, Y. K.; Slonimsky, G. L. J Polym Sci Part B: Polym Phys 1974, 12, 1053.
21. Wu, C. H.; Eder, G.; Janeschitz-Kriegl, H. Colloid Polym Sci 1993, 271, 1116.
22. Song, C. H.; Isayev, A. I. Polymer 2001, 42, 2611.
23. Van Krevelen, D. W., Ed. Properties of Polymers; Elsevier: Amsterdam, 1990.
24. Wunderlich, B. Thermal Analysis; Academic Press: Boston, 1990.
25. Chan, T. W.; Guo, L.; Isayev, A. I. SPE ANTEC Tech Pap 1995, 53, 1476.
26. Isayev, A. I.; Catignani, B. F. Polym Eng Sci 1997, 37, 1526.
27. C-MOLD. Material Properties—C-Mold Version 4.0.
28. Lide, D. R. CRC Handbook of Chemistry and Physics; CRC Press: Boca Raton, FL, 1992.
29. Isayev, A. I.; Kwon, K.; Kim, K. H. SPE Tech Pap 2006, 52, 1190.